

PROCEEDINGS OF SPIE

SPIDigitalLibrary.org/conference-proceedings-of-spie

Calibration system for mid-infrared superconducting nanowire single photon detectors

Michelle Brann, Varun Verma, Solomon Woods

Michelle R. Brann, Varun Verma, Solomon I. Woods, "Calibration system for mid-infrared superconducting nanowire single photon detectors," Proc. SPIE 12687, Infrared Sensors, Devices, and Applications XIII, 1268703 (10 October 2023); doi: 10.1117/12.2676912

SPIE.

Event: SPIE Optical Engineering + Applications, 2023, San Diego, California, United States

Calibration System for Mid-Infrared Superconducting Nanowire Single Photon Detectors

Michelle R. Brann^{*a}, Varun Verma^b, Solomon I. Woods^a

^aNational Institute of Standards and Technology (NIST), Gaithersburg, MD 20899, United States of America; ^bNational Institute of Standards and Technology (NIST), Boulder, CO 80305, United States of America

Superconducting nanowire single photon detectors (SNSPDs) have low dark counts, improved gain stability, and high resolution compared to traditional infrared detectors. Recent work at National Institute of Standards and Technology (NIST) and National Aeronautics and Space Administration (NASA) has incorporated SNSPDs into arrays and extended the response into the mid-infrared to use for spectroscopy and hyperspectral imaging. We are developing novel methods to spectrally calibrate and measure stability of these detectors in this challenging wavelength range from 3 μm to 25 μm . We present our design of a novel cryogenic apparatus uniquely focused on making quantitative efficiency measurements of these quantum detectors by directly comparing to a reference calibrated blocked-impurity-band (BIB) detector so they can be used by researchers from federal agencies, universities, and industry.

Keywords: Sensors, Calibration, Mid-IR, Superconducting, NIST

INTRODUCTION

Since the discovery that superconducting nanowires could detect single photons[1, 2] twenty years ago, this technology has been developed into superconducting nanowire single photon detectors (SNSPDs). SNSPDs have low dark count rates, improved gain sensitivity, near-unity detection efficiency, short dead times, and picosecond time resolution.[3] SNSPDs also have the advantage of operating at relatively high temperatures (1 K to 4 K) compared to transition edge sensors (100 mK) commonly used in astronomical applications. Additionally, SNSPDs have digital output signals and are thus not impacted by amplifier gain or voltage offset drifts that can cause analog signal instability.[4] Recent work focuses on increasing the efficiency, multiplexing, and extending the use of these detectors into “exotic” wavelengths such as the mid-infrared (mid-IR) and ultraviolet (UV).[5, 6]

The mid-infrared region from 2.8 μm to 25 μm is extremely important, particularly for astronomical applications and hyperspectral imaging, but vastly underexploited. This region is rich with chemical and biological signatures to help characterize conditions for habitability during the planet formation process, and to understand how galaxies evolve over time.[7] The planned Origins Space Telescope NASA mission includes a mid-infrared transit spectrometer to survey biosignatures for small rocky planets orbiting stars in their habitable zones over the range of 2.8 μm to 20 μm . [4] The current design of this spectrometer includes both HgCdTe detectors for bands up to 10 μm and blocked-impurity-band detectors (BIBs) for longer bands up to 20 μm . To accurately detect the star’s spectrum during transit for biosignature detection these spectrometers require 5×10^{-6} detector stability. Presently, BIB detectors are only able to achieve 20×10^{-6} stability.[8] SNSPDs have high sensitivity and are highly stable in the near-IR; they are a promising alternative detector for the full mid-infrared if their sensitivity and stability can be extended out to 25 μm .

We are developing novel methods to spectrally calibrate and measure stability of these detectors in this challenging wavelength range. One reason that precise measurements of SNSPDs in the mid-IR region have not been conducted yet is that there is a tremendous experimental challenge in limiting the effect of room temperature background radiation on the measurements. In recent years, SNSPDs have been calibrated out to wavelengths near 1 μm , [9] but at room temperature there are 5.6×10^{14} as many 10 μm mid-IR photons emitted as there are 1 μm photons emitted. To avoid such a high background, precise spectral calibrations of SNSPDs will need to be conducted with all parts of the spectral measurement system at cryogenic temperatures. We present our calibration system design which enables comparison of the SNSPD response with that of another cryogenic detector housed in the same cryostat. The SNSPD and calibrated Si:As BIB detector [10] are illuminated in turn by the identical free-space optical beam, enabling calibration of SNSPD counts-per-second at known powers. Our setup will provide spectral response and quantum efficiency calibrations of

these single photon detectors with well-defined uncertainties. Our measurements will help inform development and optimization of SNSPDs into arrays and will be essential for their development and ultimate implementation into future space missions and instruments where high stability, high accuracy, and low noise in the mid-infrared are essential.

SNSPD PRINCIPLES AND FABRICATION

SNSPDs are comprised of a narrow (50 nm to 100 nm) superconducting nanowire patterned from a thin film (5 nm to 10 nm) using a top-down fabrication approach. The nanowire acts as a gate valve which opens when the photon is absorbed, causing the bias current to be shunted into the amplifier and readout electronics. After the device is cooled below its superconducting transition temperature, it is biased with a constant current. When a photon is absorbed by the material, this breaks the Cooper pairs and creates a localized non-superconducting hotspot region. Over the next few picoseconds, this area spreads across the nanowire's width therefore increases the wire's resistance by ≈ 3 kilo-ohms. Since this resistance is larger than the amplifier's impedance, the bias current is transferred to the amplifier as a readout voltage pulse. When this transfer occurs, the resistive region subsides, and the wire becomes fully superconducting again.

Our SNSPD calibration cryostat is being developed in two stages for (1) measurements in near-IR (1550 nm) and for (2) measurements in the mid-IR (3 μm to 25 μm). The SNSPDs for both stages of the design process are fabricated at NIST Boulder. Near-IR SNSPDs are fabricated from MoSi[11] while mid-IR SNSPDs are fabricated from WSi[5]. Sensitivity in the mid-infrared was achieved by increasing the resistivity of the superconducting film by adjusting its stoichiometry to be Si rich ($\approx 50\%$).[5]

INITIAL DEVELOPMENT AND SNSPD MEASUREMENTS AT 1550 NM

Our first goal was to build up our cryostat to make measurements of near-infrared SNSPDs at 1550 nm and characterize these detectors through a series of optical and electrical tests. We were also able to develop device collection procedures. Our cryostat is a cryogen-free ^3He model that can reach a base temperature of 300 mK with a hold time of 30 h. The cryostat has a pulse tube cryocooler with a 40 K first stage and a second stage with a base temperature near 3 K. ^3He from a reservoir is collected in a ^3He pot, which is subsequently evaporatively cooled to its base temperature of around 300 mK by a charcoal sorption pump.

Due to their superconducting material composition and low temperature required for operation, the SNSPDs are attached to the bottom (300 mK) plate of the system. We designed two custom copper mounts: one to attach the SNSPDs to the 300 mK plate of our cryostat and one to effectively heat sink the coax cables. First, to verify that the detectors survived the transit from NIST Boulder, we measured the critical temperature of two SNSPDs. The resistivity vs. temperature measurements were made using a two-point measurement. The temperature was swept from 1.5 K to 6.0 K with the current set to 5×10^{-7} A while continuously measuring the resistance using a lock-in amplifier. This current is less than the switching current of our devices (see **Figure 2**). The normalized resistance of each device vs. temperature is plotted in **Figure 1**. The devices are superconducting with a critical temperature near 4.5 K. We also measured the resistance during the cooldown of the system and found no hysteresis in the critical temperature.

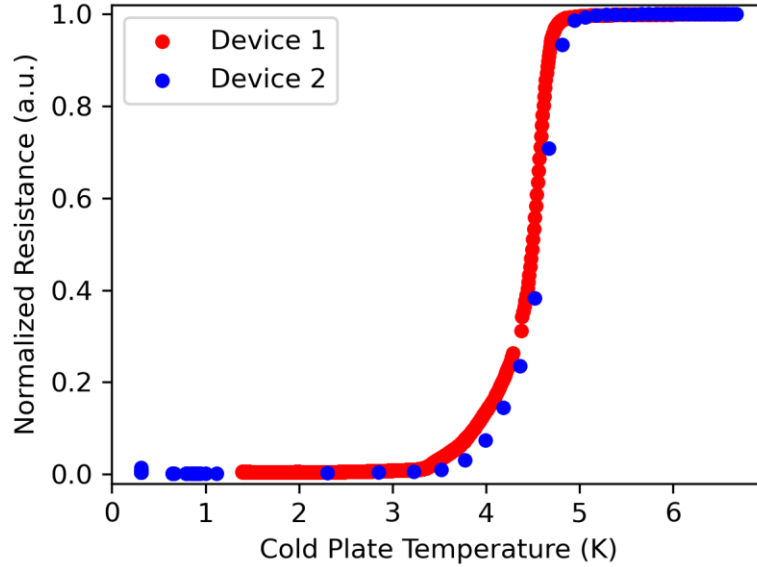


Figure 1. T_c measurement of two MoSi SNSPDs demonstrate a critical temperature near 4.5 K.

Next, we measured the current vs. voltage (I-V) curves of the devices with the device temperature at 300 mK. The I-V curves were generated using a voltage source and 100 k Ω bias resistor to generate the bias current, and a precision multimeter to readout the voltage. While sweeping the current from 0 to 10 μ A and to -10 μ A at a rate of 0.1 μ A/s, we generated I-V curves. Representative curves for both devices are plotted in **Figure 2**. We collected three independent measurements for each device and found the critical current for both devices to be 8.75 μ A.

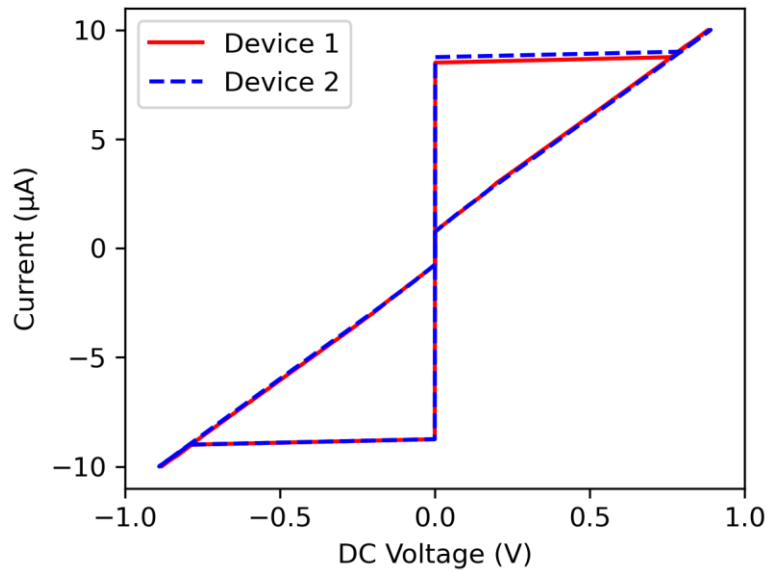


Figure 2. I-V Curves for the two near-infrared SNSPD devices at 300 mK. The critical current is 8.75 μ A.

To characterize the photon count rate of the two devices, we use a 1550 nm laser source connected to optical attenuators and commercial SMF-28 single mode patch cable. The single mode patch cable is spliced to bare SMF-28 fibers before being epoxied into a machined fiber feedthrough and entering the cryostat. We also took care to heat sink the fibers at each plate (40 K, 3 K, and 300 mK) and to baffle at each stage to avoid any stray light entering the device which would result in a higher background or impacting the bias current. The optical fibers from the feedthrough were spliced to SMF-28e+ fiber pigtailed terminated in 2.5 mm ceramic ferrules and anti-reflective coated for 1550 nm light. Thus, for 1550 nm light, our photons are fiber-coupled all the way from the laser into the devices.

To make a counts measurement, we biased the device with a low-noise direct current (DC) voltage source applied to a 100 k Ω bias resistor connected to the DC port of a bias T. Our SNSPDs were connected to the radio frequency (RF)+DC port of the bias and the RF output was connected to two low noise amplifiers that provided a gain of 46 dB. The output from the amplifiers was connected to a counter to collect SNSPD pulses. We identified individual pulses to set the trigger at 200 mV before collecting the photon count rate (PCR) and dark count rate (DCR) as a function of incident bias current (**Figure 3**). We used a gate time of 1 s for all measurements.

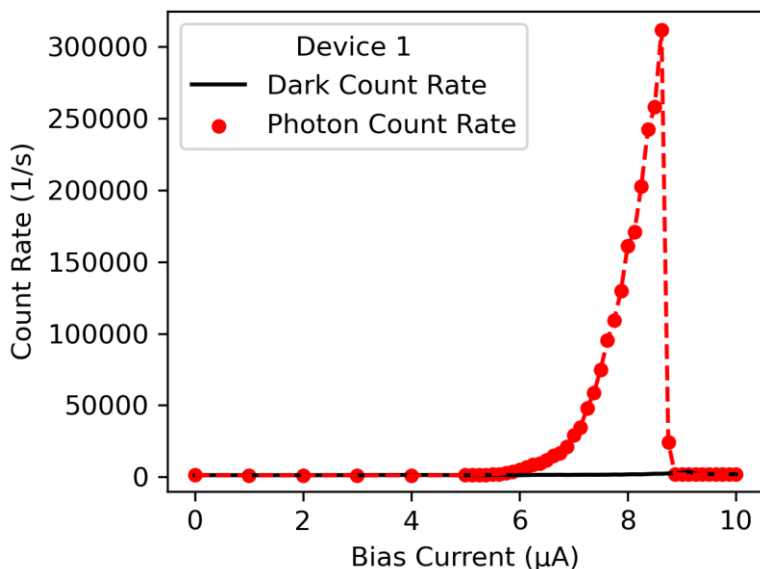


Figure 3. Photon count rate and dark count rate for a SNSPD obtained at a wavelength of 1550 nm and an operating temperature of 300 mK.

We have low dark counts (less than 3000) and see saturation of PCR at a bias count of 8.625 μA for one of our devices. We are currently in the process of collecting photon count rate curves vs. incident bias current for the second device.

We have successfully incorporated SNSPDs into our cryostat and have instituted measurement protocols for critical temperature, I-V, and PCR for the devices. We can use this knowledge and cryostat infrastructure to extend SNSPD measurements into the mid-IR, in tandem with changes to the optical circuit to enable transmission of mid-IR photons to the mid-IR SNSPDs and reference detectors. Our ultimate goal is to not only calibrate SNSPDs in the mid-IR, but to have a universal design such that we can simply adjust the incident photon wavelength and make measurements from 1550 nm to 25 μm .

DESIGN OF THE MID-IR CALIBRATION SYSTEM

We are currently building a novel cryogenic calibration system for mid-infrared-optimized SNSPDs and developing a NIST-based calibration method for mid-IR single photon detectors. Calibration in the mid-IR is noticeably more difficult than in the near-IR, where SNSPD calibration techniques are well established, since many of the components such as attenuators and reference detectors are not commercially available in the mid-IR.

In general, the SNSPD calibration will occur by comparing our SNSPD signal to a custom NIST-calibrated Si:As blocked-impurity-band (BIB) detector (traceable to an absolute cryogenic radiometer (ACR), primary reference detector). A schematic of our novel design is shown in **Figure 4**. First, we note that due to the heat load and operating temperature of the BIB detector (≈ 8 K), it is imperative that the BIB detector be mounted on the 3 K plate with standoffs. All measurements will be made in radiance mode since we are worried about background counts from our detectors due to extra stray light that occurs when flooding to make measurements in irradiance mode. Radiance is the optical power per area of the source per steradian of solid angle.[12] Our method involves an identical light path that hits

either the BIB detector or the SNSPD (using a parabolic mirror on a rotation stage). Our goal is to have ≈ 1 pW of power at each detector.

The fibers used in this calibration are multi-mode fibers that contain AgCl:AgBr in both the core and cladding material. The core diameter is 400 μm and the cladding diameter is 500 μm with an effective numerical aperture of 0.28. Our fiber transmission range is from 3 μm to 20 μm . Our first test will use a 7.7 μm quantum cascade laser on the outside of the cryostat with neutral density (ND) filters to attenuate the power, focused into a mid-IR fiber. The mid-IR optical fiber is epoxied into a vacuum feedthrough mounted at the top of the cryostat. The light from the optical fiber gets collimated at the first 90° off-axis parabolic mirror and is sent across the cryostat plate and through a bandpass filter. Then, the collimated light hits the second parabolic mirror which focuses the light directly down (SNSPD) or up (BIB) to a spot on the active area of either detector. The second parabolic mirror is on a rotational stage with a stepper motor to move the mirror by 180°. This allows both detectors to be measured during the same cooldown. In direct contrast to our near-IR setup, these fibers are free-space coupled into each device. Similar to our near-IR setup, we will need to heat sink the fibers with machined clamps at each stage in the cryostat (40 K and 3 K) to reduce heat load at the 300 mK stage and employ light-baffling to reduce stray light hitting the devices.

Due to our cryostat dimensions, we have chosen 90 degree off-axis parabolic mirrors with effective focal length (EFL) of 50.8 mm and 76.2 mm which results in a focused spot size of approximately 0.6 mm at the detectors. The second parabolic mirror EFL gives enough distance to the 3 K or 300 mK plate so that there is space to mount our custom detector attachments to the plates. Since the active area of the BIB detector is ≈ 50 times larger, this results in underfilling our BIB detector, but the SNSPD will be overfilled. By mounting the SNSPD on an XY stage with 20 mm of scanning distance in each direction, we will be able to profile the beam spot and then directly relate the power back to the BIB detector. We will also be able to account for any discrepancies between the focus point on each detector that occur from flipping the parabolic mirror. **Figure 5** provides a top view of the cryostat design to demonstrate how the XY stage and SNSPD are incorporated into the system directly underneath and 76.2 mm below the second parabolic mirror. If necessary, we can add an additional cold ND filter in front of the SNSPD to provide additional attenuation, but our first design version has identical power at each detector to avoid any additional uncertainties.

We also need to make sure that our incident radiation is carefully filtered using a cold, narrow bandpass filter. There is concern that excess blackbody radiation could exceed the maximum count rate of the detector such that the SNSPD could latch to the normal state at a bias current far below the critical current. Thus, we estimated the blackbody radiation coming from our 3 K plate that could hit the SNSPD. We first used Planck's radiation law for spectral radiance [12] for 3 μm to 25 μm radiation at 3 K and then calculated the fraction of that optical radiation which would strike the SNSPD detector on the 300 mK plate. We determined that there is no relevant mid-IR wavelength where we need to be concerned with background from our 3 K plate producing significant signal at either the SNSPD or BIB detector. However, we also calculated the temperature that would produce a signal with a count rate of 1 s^{-1} at the SNSPD from 20 μm radiation. For this calculation, we assumed that our active area of the patterned nanowires was 16 $\mu\text{m} \times 16 \mu\text{m}$ [11] and found that the temperature was about 10 K. Therefore, for our current configuration with a BIB and SNSPD we only need to be concerned about background counts impacting our device measurements if the temperature is greater than 10 K.

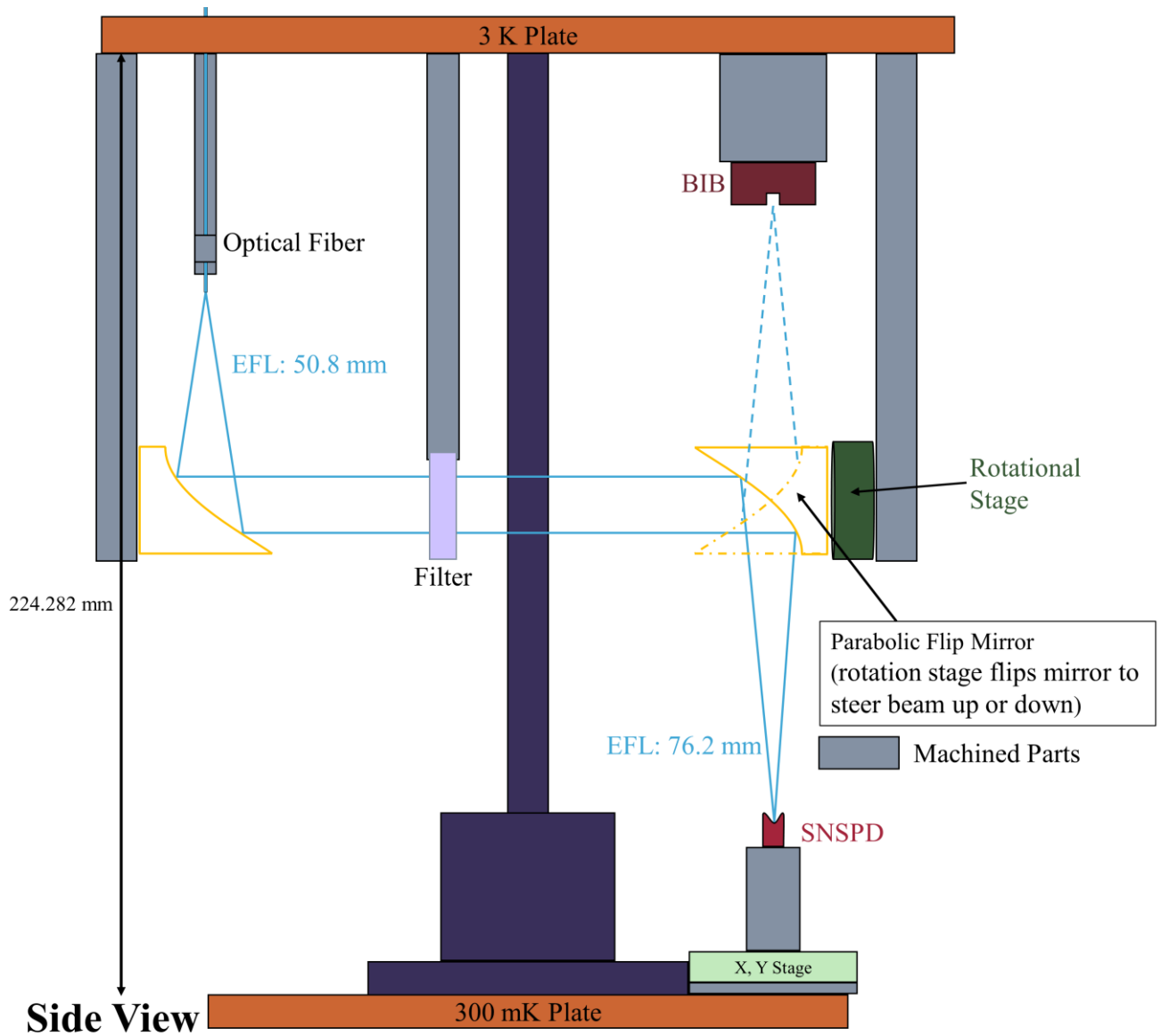


Figure 4. Side view of our novel mid-IR SNSPD calibration cryostat design. The design allows for SNSPD spectral response and quantum efficiency measurements by comparing to a calibrated BIB reference detector.

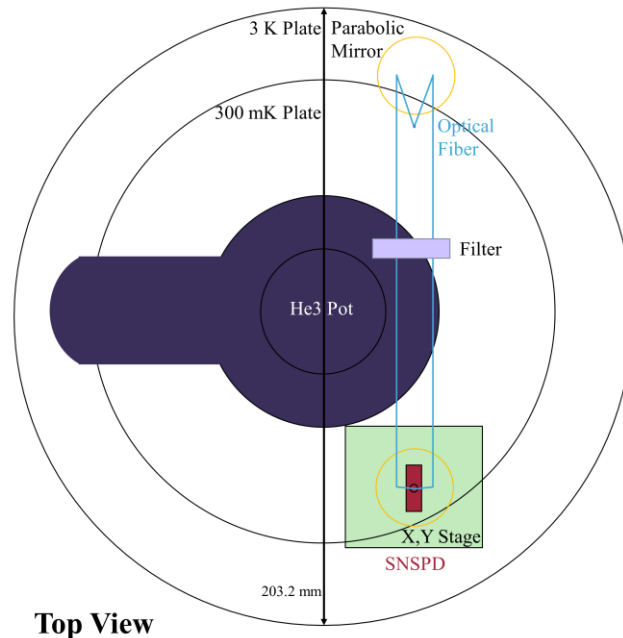


Figure 5. Top view of our novel mid-IR SNSPD calibration cryostat design. For simplicity, only the SNSPD is shown, but the BIB detector is directly on top.

The design presented here is our first iteration. We are currently using it to build up our system and make initial measurements of SNSPDs at longer wavelengths. However, we are also considering some additions that would improve our system. The first is incorporation of an integrating sphere. The integrating sphere would allow us to attenuate and adjust the beam to be more uniform. We are also interested in adding in an ACR[13] that would serve as a primary reference detector to the BIB while making SNSPD calibration measurements on a single cooldown cycle. An ACR would require additional baffles or filters, however, since a detector has responsivity at wavelengths well beyond 20 μm .

DISCUSSION AND CONCLUSION

SNSPD calibration procedures in the near-IR are well established with low uncertainties (0.7 %) for a single fiber-coupled measurement.[14] For one method developed at NIST for near-IR wavelengths, a fiber-coupled laser is coupled to a variable fiber attenuator. Traceable calibration occurs by using optical power meters that maintain their calibration at low levels. Calibration of the SNSPD device under test (DUT) occurs by employing a calibrated beam splitter and an additional reference power meter. By using optical fibers that are directly coupled to the DUT and the power meter, two unique fibers are required to make a single measurement during one cooldown cycle. Additionally, the power meter does not operate under cryogenic temperatures. This method is also dependent on the calibration of individual components and limited based on the sensitivity of the power meter.

Many of the near-IR components (attenuators, beam splitters) are not commercially available for use in the mid-IR. Thus, in our novel design (**Figure 4-5**), we incorporated ND filters to attenuate the beam. We also switched to a free-space coupled system that follows in series after a multi-mode optical fiber. This ensures that our calibrated BIB reference detector, also in the cryogenic system with an identical path from the laser source, samples the same beam as the DUT. In general, by incorporating a free-space coupled system, we will be able to make broadband spectral measurements over the entire mid-IR range.

We have presented preliminary data from our new ^3He cryostat system showing critical temperature, current-voltage, and photon count rate for near-IR SNSPDs. We have also shared a schematic of our first design that will enable measurement of SNSPDs in the mid-IR and allow for direct calibration of the devices by comparison to a calibrated BIB reference detector. Our design utilizes the same path length and beam for each detector, and by scanning the SNSPD in radiance mode we will be able to gain information about the beam spot size and spatial uniformity. Design and

construction are ongoing to make calibrations possible at these longer wavelengths and initial measurements will be made in the near future on mid-IR SNSPDs.

COMMERCIAL DISCLAIMER

We note that certain commercial equipment, instruments, and software are identified in this paper to foster understanding. Such identification does not imply recommendation or endorsement by the National Institute of Standards and Technology, nor does it imply that the materials or equipment identified are necessarily the best available for the purpose.

ACKNOWLEDGEMENTS

M.R.B thanks the National Research Council Post-Doctoral Fellowship program for supporting this work. Additional support is provided by the Air Force CCG program. We are also thankful for assistance by Thomas Gerrits, Adam McCaughan, and Chris Yung.

REFERENCES

- [1] C. M. Natarajan, M. G. Tanner, and R. H. Hadfield, "Superconducting nanowire single-photon detectors: physics and applications," *Superconductor Science and Technology*, 25(6), 1-16 (2012).
- [2] R. H. Hadfield, "Single-photon detectors for optical quantum information applications," *Nature Photonics*, 3(12), 696-705 (2009).
- [3] I. Esmail Zadeh, J. Chang, J. W. N. Los *et al.*, "Superconducting nanowire single-photon detectors: A perspective on evolution, state-of-the-art, future developments, and applications," *Applied Physics Letters*, 118(19), 190502-14 (2021).
- [4] E. E. Wollman, V. B. Verma, A. B. Walter *et al.*, "Recent advances in superconducting nanowire single-photon detector technology for exoplanet transit spectroscopy in the mid-infrared," *J. Astron. Telesc. Instrum. Syst.*, 7(1), 011004-10 (2021).
- [5] V. B. Verma, B. Korzh, A. B. Walter *et al.*, "Single-photon detection in the mid-infrared up to 10 μm wavelength using tungsten silicide superconducting nanowire detectors," *APL Photonics*, 6(5), 056101 (2021).
- [6] J. A. Lau, V. B. Verma, D. Schwarzer *et al.*, "Superconducting single-photon detectors in the mid-infrared for physical chemistry and spectroscopy," *Chemical Society Reviews*, 52(3), 921-941 (2023).
- [7] E. G. Amatucci, L. N. Allen, J. W. Arenberg *et al.*, "Origins Space Telescope: baseline mission concept," *Journal of Astronomical Telescopes, Instruments, and Systems*, 7(01), 1-23 (2021).
- [8] T. Matsuo, T. P. Greene, R. R. Johnson *et al.*, "Photometric precision of a Si: As impurity band conduction mid-infrared detector and application to transit spectroscopy," *Publications of the Astronomical Society of the Pacific*, 131(1006), 124502 (2019).
- [9] F. Marsili, V. B. Verma, J. A. Stern *et al.*, "Detecting single infrared photons with 93% system efficiency," *Nature Photonics*, 7(3), 210-214 (2013).
- [10] S. I. Woods, J. E. Proctor, T. M. Jung *et al.*, "Wideband infrared trap detector based upon doped silicon photocurrent devices," *Applied Optics* 57(18), D82-D89 (2018).
- [11] V. B. Verma, B. Korzh, F. Bussières *et al.*, "High-efficiency superconducting nanowire single-photon detectors fabricated from MoSi thin-films," *Optics Express*, 23(26), 33792 (2015).
- [12] A. C. Parr, R. Datla, and J. Gardner, [Optical radiometry] Elsevier, (2005).
- [13] S. Carr, S. I. Woods, T. M. Jung *et al.*, "PicoWatt infrared power measurement using an absolute cryogenic radiometer." 7298, 1432-1439.
- [14] T. Gerrits, A. Migdall, J. C. Bienfang *et al.*, "Calibration of free-space and fiber-coupled single-photon detectors*," *Metrologia*, 57(1), 015002 (2020).